

A thalamic input to the nucleus accumbens mediates opiate dependence

Yingjie Zhu¹, Carl F. R. Wienecke¹, Gregory Nachtrab¹ & Xiaoke Chen¹

Chronic opiate use induces opiate dependence, which is characterized by extremely unpleasant physical and emotional feelings after drug use is terminated. Both the rewarding effects of a drug and the desire to avoid withdrawal symptoms motivate continued drug use^{1–3}, and the nucleus accumbens is important for orchestrating both processes^{4,5}. While multiple inputs to the nucleus accumbens regulate reward^{6–9}, little is known about the nucleus accumbens circuitry underlying withdrawal. Here we identify the paraventricular nucleus of the thalamus as a prominent input to the nucleus accumbens mediating the expression of opiate-withdrawal-induced physical signs and aversive memory. Activity in the paraventricular nucleus of the thalamus to nucleus accumbens pathway is necessary and sufficient to mediate behavioural aversion. Selectively silencing this pathway abolishes aversive symptoms in two different mouse models of opiate withdrawal. Chronic morphine exposure selectively potentiates excitatory transmission between the paraventricular nucleus of the thalamus and D2-receptor-expressing medium spiny neurons via synaptic insertion of GluA2-lacking AMPA receptors. Notably, *in vivo* optogenetic depotentiation restores normal transmission at these synapses and robustly suppresses morphine withdrawal symptoms. This links morphine-evoked pathway- and cell-type-specific plasticity in the paraventricular nucleus of the thalamus to nucleus accumbens circuit to opiate dependence, and suggests that reprogramming this circuit holds promise for treating opiate addiction.

To systematically map brain regions that directly innervate the nucleus accumbens (NAc), we stereotactically injected a rabies virus in which the viral glycoprotein was replaced by red fluorescent protein mCherry (RV-mCherry) into the medial shell of the NAc^{10,11}. Besides well-characterized inputs to the NAc, such as the prefrontal cortex, ventral hippocampus and basolateral amygdala (BLA)^{8,10,12} (Extended Data Fig. 1a), we also detected mCherry-expressing neurons in the paraventricular nucleus of the thalamus (PVT) (Fig. 1a and Extended Data Fig. 1b). This result was particularly interesting because although previous studies have suggested a potentially important role for the PVT in drug-seeking behaviour, its underlying circuitry mechanism remains unknown^{13–15}.

To characterize the PVT to NAc connection, we injected channelrhodopsin2-expressing adeno-associated virus (AAV-ChR2) into the PVT, then prepared acute NAc slices containing ChR2-expressing terminals from the PVT¹⁶ (Extended Data Fig. 2a). Brief light stimulation (3–5 ms) elicited reliable firing of action potentials up to 20 Hz in ChR2-expressing PVT neurons (Extended Data Fig. 2b). The same stimulation also evoked robust α -amino-3-hydroxy-5-methyl-4-isoxazolepropionic acid receptor (AMPA)-mediated excitatory postsynaptic currents (EPSCs) in medium spiny neurons (MSNs), as it was blocked by bath application of a competitive AMPAR antagonist CNQX (Extended Data Fig. 2c). Light stimulation also evoked picrotoxin-sensitive inhibitory postsynaptic currents (IPSCs) (Extended Data Fig. 3b). Because the PVT contains few, if any, GABAergic neurons (Extended Data Fig. 3a), it is likely that these IPSCs were caused by

feed-forward inhibition in a local NAc circuit. Consistent with this prediction, PVT activation-evoked IPSCs had a longer delay than that of the EPSCs, and the IPSCs were blocked by CNQX (Extended Data Fig. 3c, d).

Activation of inputs from the prefrontal cortex, ventral hippocampus and BLA to the NAc is rewarding and drives self-stimulation behaviour^{8,9}. To directly assess the behavioural consequences of PVT→NAc circuit activity, we optogenetically activated this pathway in freely moving mice and examined their motivational valence using a real-time place preference assay (Fig. 1b, Methods and Extended Data Fig. 4). Strikingly, optogenetic activation of the PVT→NAc pathway reduced the time spent in the chamber paired with light stimulation (Fig. 1c). This indicates that, unlike other major inputs to the NAc, activation of the PVT→NAc pathway is aversive rather than rewarding.

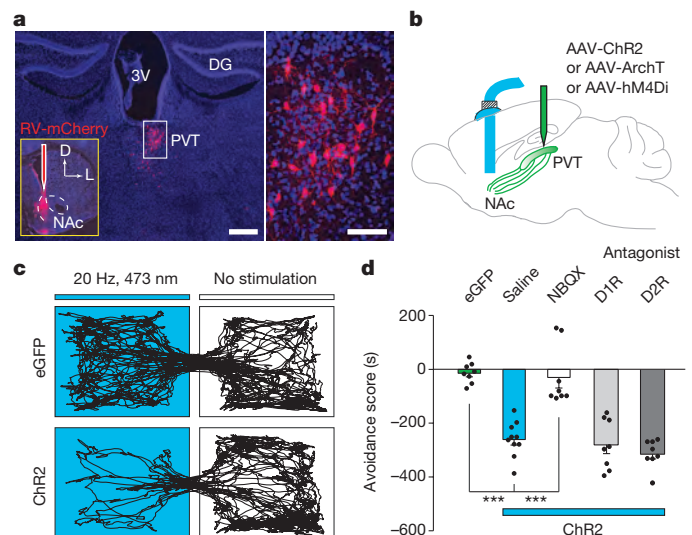


Figure 1 | *In vivo* optical activation of the PVT→NAc pathway evokes behavioural aversion. **a**, Left: cluster of retrogradely labelled cells was observed in the PVT 5 days after injection of RV-mCherry into the medial shell of the NAc ($n = 7$). Scale bar, 500 μm ; inset shows the RV-mCherry injection site. Right: magnified image shows the morphology of labelled neurons in the boxed area. Scale bar, 50 μm . D, dorsal; L, lateral; 3V, third ventricle; DG, dentate gyrus. **b**, Schematics of *in vivo* manipulation of the PVT→NAc circuit in behaving animals. **c**, Representative real-time place preference tracks illustrate light-evoked behavioural aversion in ChR2-expressing mice (bottom, $n = 10$) but not in eGFP-expressing control mice (top, $n = 8$). **d**, Quantification of light-evoked aversion and its effect by intra-NAc pharmacological manipulations. Intra-NAc infusions of NBQX (AMPA antagonist, 1.0 μg in 200 nl, $n = 8$) but not saline ($n = 10$), SCH23390 (D1R antagonist, 0.2 μg in 200 nl, $n = 8$) or raclopride (D2R antagonist, 0.3 μg in 200 nl, $n = 8$) abolished behavioural aversion evoked by optical stimulation of the PVT→NAc fibres. One-way analysis of variance (ANOVA) ($F_{(4,37)} = 29.61$, $P < 0.0001$) followed by post-hoc Tukey's test. *** $P < 0.001$. Mean \pm s.e.m.

¹Department of Biology, Stanford University, Stanford, California 94305, USA.

Avoidance of the light-paired chamber was dependent on local glutamatergic but not dopaminergic transmission in the NAc. Intra-NAc infusion of AMPAR antagonist NBQX abolished the avoidance behaviour, while intra-NAc infusion of D1 receptor (D1R) antagonist SCH23390 or D2 receptor (D2R) antagonist raclopride had no effect (Fig. 1d). These results demonstrate that the PVT→NAc pathway transmits negative valence, and reveal an input-specific mechanism driving motivated behaviour in the NAc.

Since activation of the PVT→NAc pathway evoked an aversive response, this pathway could be instrumental for the negative symptoms of drug withdrawal. To test this, we selectively silenced the pathway in two different models of opiate withdrawal and examined withdrawal-induced physical signs and place aversion. We used optogenetic terminal silencing by injecting an archaerhodopsin-3 (ArchT)-expressing AAV into the PVT and bilaterally implanting fibre guide cannulae in the NAc¹⁷ (Extended Data Fig. 4). Two weeks after surgery, mice were rendered opiate dependent via daily intraperitoneal (i.p.) injections of morphine in their home cage with doses escalating from 10 to 50 mg per kg body weight¹⁸ (Fig. 2a). Two hours after the final morphine treatment, we injected naloxone, a μ -opioid receptor antagonist (5 mg per kg body weight, i.p.), and confined the mice to one side of a two-compartment conditioned place aversion (CPA) training chamber³. This naloxone dose evoked strong negative somatic signs and robust avoidance to the withdrawal chamber in morphine-dependent mice, but not in drug-naive mice (Extended Data Fig. 5). Moreover, injection of naloxone in chronic morphine-treated mice elicited robust expression of c-Fos, a marker for recent neuronal activity, in the PVT^{NAc} projection neurons, which were labelled by injecting of retrograde tracer CTB-488 into the NAc (Fig. 2b, c and Extended Data Fig. 6a, b). Remarkably, constant bilateral optogenetic silencing of the PVT→NAc pathway during naloxone-precipitated withdrawal suppressed somatic signs of opiate dependence and learned place-aversion (measured 1 and 7 days after withdrawal) (Fig. 2d, e).

Opiate withdrawal in humans often results from cessation or reduction of opiate use, rather than blockade of opioid receptors, and this process can also be modelled in mice^{2,19}. Spontaneous opiate withdrawal also evoked expression of c-Fos in PVT^{NAc} projection neurons (Extended Data Fig. 6b, c). To measure aversive motivational states during spontaneous opiate withdrawal, mice were confined for 45 min to one side of a CPA training chamber 16 h after each morphine injection. After four training sessions, mice developed aversion to the withdrawal chamber. We employed inhibitory designer receptors exclusively activated by designer drugs (DREADD; AAV-hM4Di) to selectively silence the PVT→NAc pathway during each 45 min CPA training trial^{20,21} (Fig. 2f and Methods). Local infusion of clozapine-*N*-oxide (CNO, 3 μ M) into the NAc before each CPA training session reduced the CPA score in AAV-hM4Di but not enhanced green fluorescent protein (eGFP)-expressing AAV (AAV-eGFP) transduced mice (Fig. 2g). PVT→NAc pathway silencing had no effect on morphine-induced locomotor activity, a measure of acute psychoactive drug effects⁷ (Fig. 2h). Interestingly, the PVT→NAc circuit has roles beyond controlling the expression of physical and emotional negative states after opiate withdrawal. Mild footshock and i.p. injection of LiCl also evoked robust expression of c-Fos in PVT^{NAc} projection neurons, and silencing the pathway during conditioning suppressed the ability of either stimulus to evoke behaviour aversion (Extended Data Fig. 7).

Chronic opiate use causes profound neuroadaptive changes in the NAc^{22,23}. The NAc comprises two major subtypes of MSN, defined by the expression of either D1 or D2 dopamine receptors (D1- or D2-MSNs). D1- and D2-MSNs are proposed to play opposing roles in mediating behavioural motivation and reward learning^{24,25}, and synaptic plasticity of these MSNs appears to be causally involved in behavioural adaptations to drug addiction and chronic pain states^{6,7,26}. Since the PVT→NAc pathway transmits negative valence and mediates opiate withdrawal symptoms, we anticipated that chronic morphine exposure might cause plasticity of the PVT input selectively onto D2-MSNs.

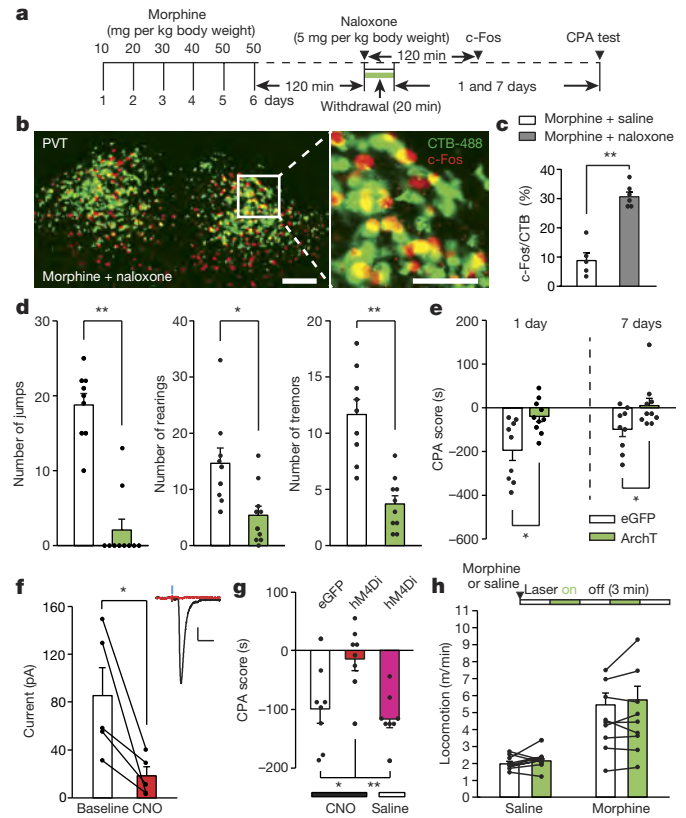


Figure 2 | The PVT→NAc pathway is required for expression of aversive withdrawal symptoms. **a**, Experimental timeline for **b–e**. **b**, Confocal images showing that naloxone-precipitated withdrawal induced robust expression of c-Fos (red) in the PVT^{NAc} projection neurons (green) that were retrogradely labelled by injection of CTB-488 into the medial shell of the NAc ($n = 6$). Left: scale bar, 100 μ m. Right: magnified image shows the boxed area; scale bar, 50 μ m. **c**, Percentage of PVT^{NAc} projection neurons expressing c-Fos. Naloxone (grey bar, $n = 6$) but not saline (white bar, $n = 5$) injection evoked significant expression of c-Fos in the PVT^{NAc} projection neurons. Mann–Whitney *U*-test. $^{**}P < 0.01$. **d**, **e**, Quantification of naloxone-precipitated withdrawal behaviours and CPA score. Light stimulation in ArchT- (green bar, $n = 10$) but not eGFP- (white bar, $n = 9$) expressing mice during withdrawal significantly reduces the number of jump, rearing and tremor events (**d**) as well as the expression of CPA (**e**). Mann–Whitney *U*-test. $^{*}P < 0.05$, $^{**}P < 0.01$. **f**, CNO (3 μ M) inhibits light-evoked synaptic current recorded from postsynaptic MSNs ($n = 5$). Inset shows example light-evoked EPSC traces before (black) and after (red) perfusion of CNO. Wilcoxon signed-rank test. $^{*}P < 0.05$. Scale bar, 20 pA, 25 ms. **g**, Spontaneous opiate withdrawal induced CPA was reduced by local infusion of CNO in hM4Di- (red, $n = 8$) but not eGFP- (black, $n = 8$) expressing mice, or local infusion of saline in hM4Di- (magenta, $n = 8$) expressing mice. One-way ANOVA ($F_{(2,21)} = 7.4$, $P < 0.01$) followed by post-hoc Tukey's test. $^{*}P < 0.05$, $^{**}P < 0.01$. **h**, Light stimulation has no effect on locomotor velocity in either saline- ($n = 9$, $P = 0.57$) or morphine- ($n = 9$, $P = 0.5$) injected animals. Wilcoxon signed-rank test. Mean \pm s.e.m.

To directly examine morphine-induced synaptic plasticity of the PVT input onto identified NAc MSNs, we prepared brain slices from transgenic animals expressing fluorescent proteins under the control of the D1R or D2R promoter, with PVT neurons infected with AAV-ChR2 (Fig. 3a). To reduce experimental variability between slices, we measured the ratio of light-evoked AMPAR-mediated EPSCs to *N*-methyl-*D*-aspartate receptor (NMDAR)-mediated EPSCs (AMPA/NMDAR ratio) in the same MSN. Consistent with our hypothesis, the escalating morphine regimen increased this ratio in D2-MSNs but not in D1-MSNs (Fig. 3b, c and Extended Data Fig. 8a, b). In contrast, presynaptic release probability was not changed in either type of MSN, as measured by the paired-pulse ratio of light-evoked EPSCs

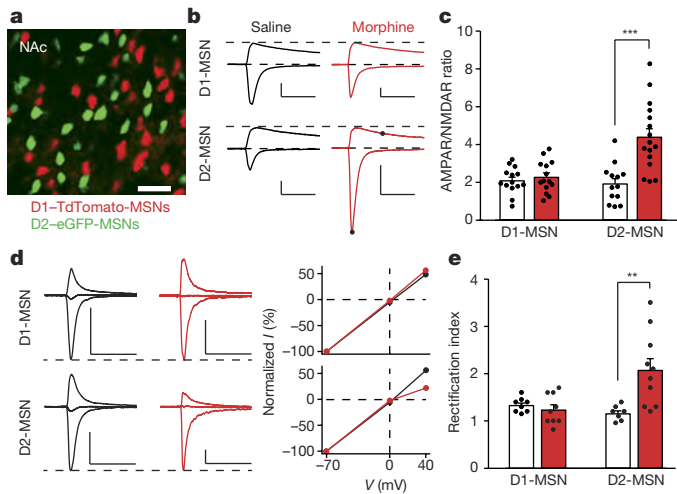


Figure 3 | Morphine-induced potentiation at the PVT→D2-MSN synapses. **a**, Image of a NAc slice from a D1-TdTomato and D2-eGFP double transgenic mouse ($n = 5$). Scale bar, 50 μm . **b**, **c**, Example traces (**b**) and quantification (**c**) of light-evoked EPSCs at -70 mV and $+40$ mV show that chronic morphine treatment significantly increased the AMPAR/NMDAR ratio in D2-MSNs (saline/morphine, $n = 13/16$ cells), but not D1-MSNs (saline/morphine, $n = 14/14$ cells). Two-way ANOVA ($F_{(1,53)} = 12.58$, $P < 0.001$) followed by post-hoc Tukey's test. $***P < 0.001$. For comparison, EPSC amplitudes are normalized to peaks at $+40$ mV. Filled dots indicate the current amplitude used for calculating the AMPAR/NMDAR ratio. Scale bar, 300 pA, 50 ms. **d**, **e**, Example traces (**d**, left), I/V curve (**d**, right) and quantification (**e**) of light-evoked AMPAR EPSCs at -70 mV, 0 mV and $+40$ mV show that morphine treatment selectively increased the rectification index of AMPAR EPSCs in D2-MSNs (saline/morphine, $n = 7/10$ cells), but not D1-MSNs (saline/morphine, $n = 8/9$ cells). Two-way ANOVA ($F_{(1,30)} = 9.87$, $P < 0.01$) followed by post-hoc Tukey's test. $***P < 0.01$. For comparison, amplitudes of AMPAR EPSCs are normalized to peaks at -70 mV. Scale bar, 250 pA, 50 ms. Mean \pm s.e.m.

in morphine-dependent mice (Extended Data Fig. 9). These results suggested that chronic morphine treatment caused a change in postsynaptic function. One plausible mechanism of drug-induced postsynaptic change is the insertion of GluA2-lacking calcium-permeable AMPAR (CP-AMPA) in the affected NAc synapses²⁷. Compared with other AMPARs, CP-AMPA has a larger conductance and show inward rectification at positive membrane potentials. In morphine-treated mice, we observed a significant increase in the rectification index selectively at PVT→D2-MSN synapses, but not at PVT→D1-MSN synapses (Fig. 3d, e). Interestingly, the AMPAR/NMDAR ratio at BLA→NAc synapses, which are part of a pathway that drives reward-seeking behaviour, was not changed by the same morphine treatment (Extended Data Fig. 8c–e). Collectively, these results indicate that the morphine regimen strengthened the PVT input selectively onto D2-MSNs via synaptic insertion of CP-AMPA.

If morphine-induced potentiation of the PVT→D2-MSN synapses is essential for the expression of opiate withdrawal symptoms, then depotentiating these synapses *in vivo* to restore its normal transmission should relieve those symptoms. To test this prediction, we employed long-term depression (LTD)-based *in vivo* manipulation of the PVT→D2-MSN synapses by photostimulating ChR2-expressing PVT terminals in the NAc at 1 Hz for 15 min^{6,7,28} (Fig. 4a). We applied this *in vivo* optogenetic LTD induction protocol in chronic morphine-treated mice, then prepared NAc slices to record photocurrents on visually identified D1- and D2-MSNs. Indeed, this light treatment reduced the AMPAR/NMDAR ratio, and rectified the AMPAR current at PVT→D2-MSN synapses to a level comparable to baseline transmission, but did not change the paired-pulse ratio (Fig. 4b–e and Extended Data Figs 8 f, g and 9). Treating morphine-dependent mice with this optogenetic LTD protocol 45 min before naloxone injection

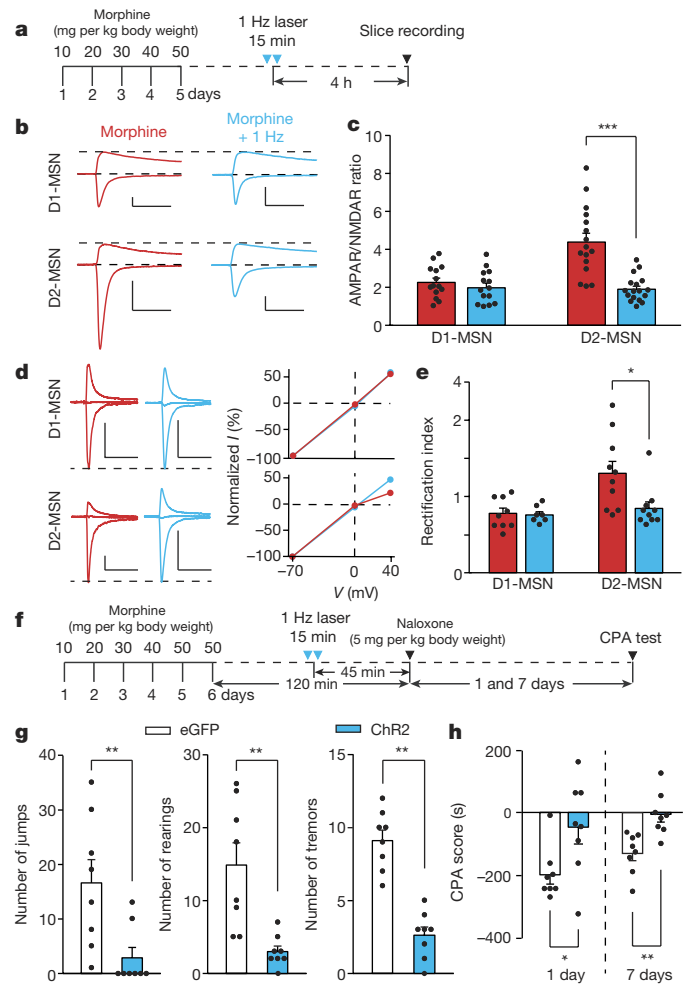


Figure 4 | *In vivo* optogenetic LTD induction restores normal transmission at PVT→D2-MSN synapses and suppresses withdrawal symptoms. **a**, Experimental timeline for **b**–**e**. **b**–**e**, *In vivo* 1 Hz photostimulation successfully normalized morphine-induced changes of AMPAR/NMDAR ratio and rectification index in D2-MSNs, but had little effect on D1-MSNs. **b**, **c**, AMPAR/NMDAR ratio of D2-MSNs (morphine/morphine + 1 Hz, $n = 16/17$ cells) and D1-MSNs (morphine/morphine + 1 Hz, $n = 14/14$). Two-way ANOVA ($F_{(1,57)} = 13.86$, $P < 0.001$) followed by post-hoc Tukey's test. $***P < 0.001$. **d**, **e**, Rectification index for AMPAR EPSCs in D2-MSNs (morphine/morphine + 1 Hz, $n = 10/10$) and D1-MSNs (morphine/morphine + 1 Hz, $n = 9/7$). Two-way ANOVA ($F_{(1,32)} = 4.3$, $P < 0.05$) followed by post-hoc Tukey's test. $*P < 0.05$. Scale bars, 300 pA, 50 ms (**b**); 250 pA, 50 ms (**d**). **f**, Experimental timeline for **g**, **h**. **g**, **h**, Quantification of withdrawal behaviours (**g**) and CPA score (**h**). In ChR2- (blue bar, $n = 8$) but not eGFP- (white bar, $n = 8$) expressing mice, *in vivo* 1 Hz stimulation suppressed naloxone-precipitated jumping, rearing and tremor events (**g**), and suppressed CPA to the withdrawal chamber (**h**). Mann-Whitney U -test. $*P < 0.05$, $***P < 0.01$. Mean \pm s.e.m.

(Fig. 4f) reduced the immediate expression of withdrawal behavioural symptoms and the aversive memory of the withdrawal chamber (Fig. 4g, h). This 1 Hz optogenetic stimulation had no effect on the plasticity at PVT→D1-MSN synapses (Fig. 4b–e). Together, these results establish a causal link between plasticity at PVT→D2-MSN synapses and the negative somatic and motivational states that accompany opiate withdrawal.

Complementary to previous studies that highlight the contribution of the prefrontal cortex, BLA, and ventral hippocampus inputs to the NAc in mediating drug reward and their plasticity onto D1-MSNs after chronic drug exposure, here we show that the PVT input transmits negative valence and its plasticity at PVT→D2-MSN synapses is necessary for the expression of aversive states associate with opiate withdrawal.

We further demonstrate that optogenetic restoration of normal synaptic transmission at these synapses effectively relieves withdrawal symptoms. Our optogenetic LTD protocol may inspire the development of novel treatments for opiate addiction involving deep brain stimulation to induce plasticity at relevant synapses²⁹.

Online Content Methods, along with any additional Extended Data display items and Source Data, are available in the online version of the paper; references unique to these sections appear only in the online paper.

Received 14 March; accepted 23 December 2015.

Published online 3 February 2016.

- Koob, G. F. & Le Moal, M. Drug abuse: hedonic homeostatic dysregulation. *Science* **278**, 52–58 (1997).
- Vargas-Perez, H., Ting-A-Kee, R. A., Heinmiller, A., Sturgess, J. E. & van der Kooy, D. A test of the opponent-process theory of motivation using lesions that selectively block morphine reward. *Eur. J. Neurosci.* **25**, 3713–3718 (2007).
- Wikler, A. A theory of opioid dependence. *NIDA Res. Monogr.* **30**, 174–178 (1980).
- Harris, G. C. & Aston-Jones, G. Involvement of D2 dopamine receptors in the nucleus accumbens in the opiate withdrawal syndrome. *Nature* **371**, 155–157 (1994).
- Koob, G. F., Wall, T. L. & Bloom, F. E. Nucleus accumbens as a substrate for the aversive stimulus effects of opiate withdrawal. *Psychopharmacology* **98**, 530–534 (1989).
- Pascoli, V. *et al.* Contrasting forms of cocaine-evoked plasticity control components of relapse. *Nature* **509**, 459–464 (2014).
- Pascoli, V., Turiault, M. & Lüscher, C. Reversal of cocaine-evoked synaptic potentiation resets drug-induced adaptive behaviour. *Nature* **481**, 71–75 (2012).
- Britt, J. P. *et al.* Synaptic and behavioral profile of multiple glutamatergic inputs to the nucleus accumbens. *Neuron* **76**, 790–803 (2012).
- Stuber, G. D. *et al.* Excitatory transmission from the amygdala to nucleus accumbens facilitates reward seeking. *Nature* **475**, 377–380 (2011).
- Lim, B. K., Huang, K. W., Grueter, B. A., Rothwell, P. E. & Malenka, R. C. Anhedonia requires MC4R-mediated synaptic adaptations in nucleus accumbens. *Nature* **487**, 183–189 (2012).
- Wickersham, I. R., Finke, S., Conzelmann, K. K. & Callaway, E. M. Retrograde neuronal tracing with a deletion-mutant rabies virus. *Nature Methods* **4**, 47–49 (2007).
- Sesack, S. R. & Grace, A. A. Cortico-basal ganglia reward network: microcircuitry. *Neuropsychopharmacology* **35**, 27–47 (2010).
- Martin-Fardon, R. & Boutrel, B. Orexin/hypocretin (Orx/Hcrt) transmission and drug-seeking behavior: is the paraventricular nucleus of the thalamus (PVT) part of the drug seeking circuitry? *Front. Behav. Neurosci.* **6**, 75 (2012).
- Browning, J. R., Jansen, H. T. & Sorg, B. A. Inactivation of the paraventricular thalamus abolishes the expression of cocaine conditioned place preference in rats. *Drug Alcohol Depend.* **134**, 387–390 (2014).
- James, M. H. *et al.* Cocaine- and amphetamine-regulated transcript (CART) signaling within the paraventricular thalamus modulates cocaine-seeking behaviour. *PLoS ONE* **5**, e12980 (2010).
- Boyden, E. S., Zhang, F., Bamberg, E., Nagel, G. & Deisseroth, K. Millisecond-timescale, genetically targeted optical control of neural activity. *Nature Neurosci.* **8**, 1263–1268 (2005).
- Chow, B. Y. *et al.* High-performance genetically targetable optical neural silencing by light-driven proton pumps. *Nature* **463**, 98–102 (2010).
- Vanderschuren, L. J. *et al.* Morphine-induced long-term sensitization to the locomotor effects of morphine and amphetamine depends on the temporal pattern of the pretreatment regimen. *Psychopharmacology* **131**, 115–122 (1997).
- Bechara, A., Nader, K. & van der Kooy, D. Neurobiology of withdrawal motivation: evidence for two separate aversive effects produced in morphine-naive versus morphine-dependent rats by both naloxone and spontaneous withdrawal. *Behav. Neurosci.* **109**, 91–105 (1995).
- Stachniak, T. J., Ghosh, A. & Sternson, S. M. Chemogenetic synaptic silencing of neural circuits localizes a hypothalamus–midbrain pathway for feeding behavior. *Neuron* **82**, 797–808 (2014).
- Armbruster, B. N., Li, X., Pausch, M. H., Herlitze, S. & Roth, B. L. Evolving the lock to fit the key to create a family of G protein-coupled receptors potently activated by an inert ligand. *Proc. Natl Acad. Sci. USA* **104**, 5163–5168 (2007).
- Williams, J. T., Christie, M. J. & Manzoni, O. Cellular and synaptic adaptations mediating opioid dependence. *Physiol. Rev.* **81**, 299–343 (2001).
- Hyman, S. E., Malenka, R. C. & Nestler, E. J. Neural mechanisms of addiction: the role of reward-related learning and memory. *Annu. Rev. Neurosci.* **29**, 565–598 (2006).
- Kravitz, A. V., Tye, L. D. & Kreitzer, A. C. Distinct roles for direct and indirect pathway striatal neurons in reinforcement. *Nature Neurosci.* **15**, 816–818 (2012).
- Lobo, M. K. *et al.* Cell type-specific loss of BDNF signaling mimics optogenetic control of cocaine reward. *Science* **330**, 385–390 (2010).
- Schwartz, N. *et al.* Decreased motivation during chronic pain requires long-term depression in the nucleus accumbens. *Science* **345**, 535–542 (2014).
- Conrad, K. L. *et al.* Formation of accumbens GluR2-lacking AMPA receptors mediates incubation of cocaine craving. *Nature* **454**, 118–121 (2008).
- Lee, B. R. *et al.* Maturation of silent synapses in amygdala–accumbens projection contributes to incubation of cocaine craving. *Nature Neurosci.* **16**, 1644–1651 (2013).
- Creed, M., Pascoli, V. J. & Lüscher, C. Refining deep brain stimulation to emulate optogenetic treatment of synaptic pathology. *Science* **347**, 659–664 (2015).

Acknowledgements We thank R. C. Malenka, K. Shen, L. Luo, T. R. Clandinin and members of the Chen laboratory for comments on the manuscript. We thank M. Asaad, J. Charalel and X. Sun for tracing and behaviour experiments. This work was supported by grants from The Whitehall Foundation, the Ajinomoto innovation alliance program, the Terman Scholarship and start-up funding from Stanford University. G.N. is supported by a training grant from the National Institute on Drug Abuse (5T32DA035165-02).

Author Contributions X.K.C. conceived the study. Y.J.Z., G.N. and X.K.C. designed the experiments. Y.J.Z. and C.F.R.W. conducted experiments. Y.J.Z. and X.K.C. analysed data. G.N., Y.J.Z. and X.K.C. wrote the manuscript, and all authors participated in the revision of the manuscript.

Author Information Reprints and permissions information is available at www.nature.com/reprints. The authors declare no competing financial interests. Readers are welcome to comment on the online version of the paper. Correspondence and requests for materials should be addressed to X.K.C. (xkchen@stanford.edu).